Marine Environmental Research 204 (2025) 106924

Contents lists available at ScienceDirect

Marine Environmental Research

journal homepage: www.elsevier.com/locate/marenvrev

Multifactored accelerated marine corrosion of immersed steels influenced by washed ashore *Sargassum* rafts

Diana Bénuffé [a], Fatima Radouani [a,1], Maxence Quemener [b], Olivia Ozier [a], Marilyne Fauchon [b], Yannick Toueix [b], Fabienne Faÿ [c], Anthony Magueresse [d], Benoit Lescop [e], Stéphane Rioual [e], Pascal Zongo [a], Christophe Roos [a], Claire Hellio [b], Paule Salvin [a,*]

[a] L3MA UR4_1 UFR STE Universite des Antilles, Campus de Schoelcher, Schoelcher, 97275, France
[b] Univ Brest, CNRS, IRD, Ifremer, LEMAR, IUEM, F-29280 Plouzane, France
[c] Laboratoire de Biotechnologie et Chimie Marines, Université Bretagne Sud, EMR CNRS 6076, IUEM, 56100, Lorient, France
[d] IRDL, CNRS 6027, Université Bretagne Sud, 56100, Lorient, France
[e] Lab-STICC, UMR CNRS 6285, Université de Bretagne Occidentale, 29200, Brest, France

ARTICLE INFO

Keywords:
Marine corrosion
Sargassum
Carbon steel
Stainless steel
Hydrogen sulphide
Biocorrosion

ABSTRACT

Since 2011, massive strandings of *Sargassum* (brown alga) have significantly affected Caribbean islands causing major health, environmental and economic problems. Amongst them, the degradation of algae releases corrosive gases, hydrogen sulphide (H_2S) and ammonia (NH_3) which causes an accelerated corrosion of the metallic structures of these coastal areas. The aim of this study was to quantify the impact of *Sargassum* strandings on the corrosion of three types of steels (DC01 carbon steel, 304L and 316L stainless steels) immersed for up to 120 days at various sites in Martinique which were gradually impacted by *Sargassum*. A multidisciplinary approach was developed, incorporating: (i) surface analysis through macrophotography and corrosion product examination, (ii) weight loss measurements, and (iii) analysis of physicochemical parameters alongside microbial composition. As a result, in the presence of degraded *Sargassum*, an anaerobic, reducing and more acidic environment was correlated with high corrosion rates for all studied steels. When high density of *Sargassum* sp. was present, elemental sulphur was identified in the corrosion product layers of DC01 and 316L. Moreover, in this condition, sulphate-reducing bacteria (SRB) were observed in the surface biofilms of 304L coupons such as *Desulfobulbus rhabdoformis*. All these factors have highlighted the aggressiveness of the medium resulting from the presence of decomposing *Sargassum*, leading to increased corrosion rates. Our work provides new information on the importance of managing *Sargassum* strandings in order to avoid accelerated degradation of metallic structures in harbours and coastal zones.

1. Introduction

Steels are widely used in industries, ships, platforms, marine structures and cooling plants in coastal environments (Ruiz-Luna et al., 2019; Sun et al., 2020). Due to numerous physicochemical, mechanical and biological processes, these environments are known to be active and aggressive media for steels (Creus et al., 2004; Javaherdashti, 2008). Marine corrosion results from abiotic factors, including chloride ions, pH, redox potential, dissolved gases like dissolved oxygen (DO), salinity, and temperature (James and Hattingh, 2015; Phull, 2010). Additionally, biotic factors, such as living organisms (e.g., sulphate-reducing bacteria (SRB)), can also influence these abiotic conditions (Daille et al., 2020; Usher et al., 2014). In seawater composition, chloride ions are considered as the most corrosive species for steels (Enning et al., 2012; Ghosh and Kain, 2010), typically causing localised corrosion or weakening the protective properties of the oxides layer. The chloride ions are adsorbed by the oxide film and react with iron to form iron chlorides increasing the anodic zones. Regarding pH, it refers to the concentration of hydrogen ions which can enhance steel corrosion by hydrogen depolarization (Butko et al., 2017). However, the calcium carbonate balance has a role of buffer in seawater maintaining the pH between 7.3 and 8.6 (Pusparizkita et al., 2023). This balance is dependent on bicarbonates,

* Corresponding author.
E-mail address: paule.salvin@univ-antilles.fr (P. Salvin).
[1] Present address: Laboratoire PC2E, UR5_3, CHU de la Martinique, 97200 Fort de France, Martinique.

https://doi.org/10.1016/j.marenvres.2024.106924
Received 19 July 2024; Received in revised form 12 December 2024; Accepted 20 December 2024
Available online 22 December 2024

carbonates, borates (Phull, 2010) and temperature permitting a constant partial pressure of CO_2 (pCO_2) (Bates and Johnson, 2020). An increase in this pressure due to high biological processes causes carbonate dissolution resulting in an acidification of the water and accelerated steel dissolution (Jin et al., 2014). Redox potential depends on factors, such as pH and DO and gives information on the redox form of the chemical species (oxidised or reduced form) in the medium (Zou et al., 2011). Moreover, high DO induces the dissolution of iron and allows the formation of corrosion products such as iron oxides, exposing steels to a pitting or uniform corrosion. On the contrary, by promoting the formation of stable layers of corrosion products, anoxic conditions can inhibit corrosion (Ruiz-Luna et al., 2019).

Other parameters such as the presence (and concentration) of nutrients (phosphorus, nitrates, ammonium) have an impact on corrosion phenomena by influencing the growth of marine organisms and the biological colonisation of the surface (Bunet, 2020; Daille et al., 2020; Melchers, 2004). Colonisation of artificial surfaces by pioneer bacterial species initiates biofouling (Lee et al., 2008). These bacteria form a primary biofilm, due to the availability of macromolecules (glycoproteins, proteins, organic matter) adsorbed to the metal surface and the secretion of extracellular polymeric substances (EPS). This organised structure allows the attachment and the protection of several types of microorganisms such as microalga (Antunes et al., 2019). It can influence metal properties by facilitating, initiating or accelerating corrosion processes at metal-electrolyte interfaces. This phenomenon is described as microbially influenced corrosion (MIC) or biocorrosion (Arroussi et al., 2022; Bermont-Bouis et al., 2007; Boudaud et al., 2010; Vastra et al., 2016). It causes significant industrial and environmental damages (Benaïssa, 2004; Bunet, 2020a). In this phenomenon, a large diversity of microorganisms (bacteria) is involved such as SRB associated with iron-oxidising bacteria (IOB) (Starosvetsky et al., 2008), sulphide-oxidising bacteria (SOB) (Brock and Gustafson, 1976) and acid producing bacteria (APB) (Beech and Sunner, 2004; Enning et al., 2012) (Table 1). SRBs are characterised by anaerobic respiration, iron as electron donor and sulphates as electron acceptors (Enning and Garrelfs, 2014). As a result of the reduction of sulphates, various sulphurous species can be formed, in particular H_2S. Instead, IOB are able to oxidise iron (II) to iron (III) which can accumulate in ochre-like deposits of insoluble iron oxides and oxyhydroxides (Hedrich et al., 2011). APB can oxidise organic or non-organic matter to produce some acids such as acetic acid, sulphuric acid attacking the steel (Javaherdashti, 2008).

Since 2011, massive strandings of brown alga *Sargassum*, known as 'golden tides', have significantly affected Caribbean islands (Smetacek and Zingone, 2013) causing major health, environmental and economic problems (Oviatt et al., 2019; Resiere et al., 2021; van Tussenbroek et al., 2017). The strandings are mainly composed of *Sargassum natans* var. *natans*, *Sargassum natans* var. *wingei* and *Sargassum fluitans* var. *fluitans* (Siuda et al., 2024). In the open sea, *Sargassum* rafts play an important ecological role by serving as habitats, nurseries or food sources for fish, turtles, crabs and other crustaceans (Martin et al., 2021; Theirlynck et al., 2023). In coastal environments, the presence of thick *Sargassum* rafts reduce the penetration of the light, increase the oxygen demand due the alga degradation and the increase of organic matter available and release organic-matter rich leachates (composed of lactic acid, methane, ammonium and phosphorus in high levels) after degradation (Cabanillas-Terán et al., 2019; van Tussenbroek et al., 2017). Moreover, the decomposition of washed ashore *Sargassum* releases toxic and corrosive gases such as hydrogen sulphide (H_2S) and ammoniac (NH_3) and heavy metals (Gray et al., 2021; Mendez-Tejeda et al., 2019; Olguin-Maciel et al., 2022). H_2S is known to cause severe pitting in pipelines due to the formation of iron sulphides, forming a non-solid protective film on steels (Choi et al., 2011; Marchal, 1999) and sulphuric acid (from oxidation of H_2S) (Dvoracek, 2013). NH_3 in presence of water can cause stress corrosion cracking to carbon steels (Latosov et al., 2017). All these conditions lead to a harmful environment with eutrophication-like conditions and modification of physicochemical parameters inducing acidification and hypoxia in coastal areas (Antonio-Martínez et al., 2020; López-Contreras et al., 2022; Oviatt et al., 2019).

All this knowledge about marine corrosion leads us to hypothesise that the conditions created by the *Sargassum* rafts washed up on the Caribbean coasts would favour the accelerated corrosion of steels. Some studies dealt with the seasonal distribution of *Sargassum* (Brooks et al., 2018; Gower et al., 2013), the effect of *Sargassum* strandings on marine fauna (Olguin-Maciel et al., 2022), microbial composition of *Sargassum* rafts (Theirlynck et al., 2023), but our work is the first investigating the impact of high density of macroalgae on marine steel corrosion. The aim of this study is to qualify and to quantify the influence of the *Sargassum* rafts on the corrosion process in seawater and to define the main abiotic and biotic factors involved. Indeed, the exposed materials were DC01 carbon steel (CS), 304L stainless steel (SS) and 316L (SS). A multidisciplinary approach was used to evaluate the marine corrosion: (i) surface analyses (macrophotography, confocal microscopy, SEM-EDS) to identify the corrosion products and their localisation in the layer of the metallic coupon surfaces, (ii) weight loss methods to study the corrosion kinetics, (iii) microbial composition analysis (metagenomics, isolation and culture) to evaluate the involvement of bacteria in the corrosion process. A possible correlation between the variation of the seawater physicochemical parameters, the presence of *Sargassum* and the corrosion kinetics was as well investigated.

Table 1
Examples of bacterial metabolisms involved in corrosion processes.

Metabolism-based group	Respiration mode	Examples of bacterial species	Mechanisms implied in the corrosion process
Sulphate-reducing bacteria (SRB)	Obligate anaerobes	*Desulfovibrio* sp. (Černoušek et al., 2020)	reduction of sulphur compounds to H_2S and reaction with Fe^{2+} to form iron sulphides
Iron-oxidising bacteria (IOB)	Aerobes	*Acidithiobacillus ferrooxidans* (Wang et al., 2014)	oxidation of iron to iron hydroxide can cause pitting corrosion.
Sulphate-oxidising bacteria (SOB)	Aerobes	*Thiobacillus thiooxidans* (Brock and Gustafson, 1976)	oxidation of sulphur compounds using Fe^{3+} to sulphuric acid which attacks the steel
Acid-producing bacteria (APB)	Aerobes/ facultative anaerobes	*Clostridium aceticum* (Little and Lee, 2007)	production of acids such as acetic acid from fermenting organic matter and promotion of iron dissolution

2. Materials and methods

2.1. Exposure sites

Three sites were selected on the Atlantic coast of Martinique (which is the most affected by *Sargassum* strandings) (Fig. S1). All sites were located in urban areas and protected from the swell. Estimation of *Sargassum* coverage on seawater surface was performed by analysing 1 m^2 from pictures of each site taken the same day. ImageJ software was used to apply black and white filters, black for non-covered surface, white for objects (*Sargassum*) at the surface of the water. The goal was to expose coupons in zones with different alga cover. The first selected site is Port of Marigot (PM) (14° 49′27.0″N 61°01′54.6″W), which is highly exposed to *Sargassum* strandings (61% of surface coverage). It is located in an area protected from the swell by a stone dike protecting the quay. The dike prevents the algae from circulating. It traps them in place, where they can rot causing the seawater to turn brown. H_2S weekly concentrations reach up to 10 ppm in the air in the vicinity of the samples measured with a Dräger sensor.

The second site is Cosmy (Co) (14° 45′10.1″N 60°58′03.3″W), which consists of a beach in a calm and sheltered bay. It has mainly a clear cover of stranded alga. A floating dam located at 100 m from the coupons is present, providing a barrier preventing alga from reaching the exposure zone.

The third site is Frégate Est 2 (FE) (14°36′30″N 60°52′29″W) which is a calm bay frequently covered with *Sargassum* rafts (71% of surface covered) composed of fresh alga. Samples were attached on a pontoon, into the fresh algae rafts.

PM and FE sites were used to compare coupons immersed respectively in decomposed *Sargassum* with those immersed in fresh *Sargassum* rafts. Temperature, pH, redox potential and salinity were measured in triplicate directly at each site with a portable multi-parameter sensor (Hi98194 pH/EC/DO multiparameter Hannainstruments®). Measurements were taken 3 to 4 times per trimester.

2.2. Steels

In this study, three types of steels were used: carbon steel DC01 (composition: C: 0.12%; Si: 0.60%; Mn:0,05%; P: 0.05%; Ti: 0.01%; Fe: cpl.), stainless steel 304L (composition: C: 0.02%; Si: 0.37%; Mn: 1.44%; P: 0.03%; S: 0.003%; N: 0.04%; Cr: 18.0%; Ni: 8.05%; Fe: cpl.) (supplier: SMGM, Martinique) and stainless steel 316L (composition: C: <0.03%; Si: 0.2%; Mn: 2.0%; P: 0.05%; S: 0.02%; N: 0.1%; Cr:18,5%; Ni: 8.1%; Mo: <2.5%; Fe: cpl.) (supplier: Top Martinique, Martinique). Steels selection was based on corrosion resistance and on its use in maritime structures (Creus et al., 2004; Phull, 2010). CS as DC01 is characterised by a high carbon content, whereas SS as 304L is characterised by a low carbon content and a high chromium content. The presence of chromium allows the formation of a chromium-rich oxide protective film on the SS surface (Jin et al., 2014). DC01 is a steel commonly used in industry for its good bending properties, but it is not resistant to corrosion. SS 304L and SS 316L are widely used in marine applications for fittings and components for boats, platforms. These metals are austenitic SS and have good ductility, strength, non-magnetic properties, weldability and a high resistance to generalised corrosion but are susceptible to localised corrosion (Gudić et al., 2023). Each coupon consisted of a 25×40 mm rectangle, 1 mm thick. A 3-mm diameter hole was drilled at each edge. The coupons were manually polished with a series of silicon carbide papers (80, 320, 500, 800, 1200 grit) using a grinding machine (Labosystem Struers®). The stainless steels were then chemically cleaned with a 20% nitric acid solution for 20 min (Trigodet et al., 2019a). Afterwards, the coupons were rinsed twice in distilled water, then in an absolute alcohol bath and dried with paper. This step allowed the coupons to be in the same physicochemical conditions. Carbon steel coupons were degreased with absolute ethanol and dried before experiment (Kuang et al., 2007).

2.3. Experimental devices and exposure times

Coupons were attached to a 610×310 mm stainless steel frame with nylon thread and double sleeves allowing them to be exposed *in situ*. The coupons are spaced 5 cm apart. The frames were placed in the tidal zone, where it has been reported in the literature that the conditions lead to an accelerated low water corrosion (ALWC), responsible for important steel degradation processes (Campbell and Beech, 2009; Smith et al., 2019). Due to the carbon steels fast rate of degradation, DC01 coupons were immersed for a maximum of 60 days while 304L and 316L coupons were immersed for 120 days. After 60 days, only a bulk of corrosion products was left on CS coupons. DC01 coupons were sampled after 0, 7, 15, 30 and 60 days and 316L coupons were sampled after 0, 7, 15, 30, 120 days and 304L coupons after 0, 7, 60, 90, 120 days. Duplicates of coupons were used for elemental composition of surface layer (DC01), for X-ray diffraction analysis (DC01 and 316L), for biofilm biovolume estimation (304L), for weight loss (DC01 and 304L) and for bacterial community analysis (DC01 and 304L).

2.4. Structural and surface characterization

2.4.1. Macroscopic observations

Macrophotographs of the steels were taken after each immersion time on a sheet of paper with a 0.5 cm grid in the laboratory after sampling in duplicat. Criteria used to compare coupons were: presence and organisation of corrosion products, colour of the surface layer (black, orange, colourless), aspect of the surface (smooth or rough), presence of macrofouling (algae, invertebrates (barnacles)).

2.4.2. EDS and X-ray diffraction

The distribution and composition of the elements formed on the surface of DC01 were analysed by energy dispersive spectroscopy (EDS) coupled to a scanning electron microscope. After sampling, coupons were immediately fixed in a 4% formaldehyde seawater buffered solution overnight at 4 °C. Then, they were rinsed 3 times in a phosphate buffer (pH = 7.2; 10 min) and dried overnight at room temperature (26 °C).

X-ray diffraction was useful to identify crystal phases in corrosion products layer of steel coupons (DC01 and 316L) (Refait et al., 2013). Non-fixed coupons were dried at room temperature and exposed to X-ray beams emitting Cu-Kα (1.5408 Å) using an Empyrean PANalytical diffractometer.

2.5. Weight loss measurements

The corrosion rate was calculated for different exposure times (7, 15, 30, 60, 90, 120 days). Clean coupons were weighed prior to exposure.

A duplicate of CS coupons for each sampling time was first sonicated (Elmasonic P 300 H, Elma Schmidbauer GmbH, frequency 37Hz, Germany) in a 10% hydrochloric acid solution bath for 30s, then in 20s increments until a stable weight was obtained. Between each sonication, the coupons were rinsed in 3 distilled water baths, dried with paper and weighed on a precision scale.

For SS coupons, duplicates were treated as above except that the coupons were cleaned in a 10% nitric acid solution bath for 20 min. A correction factor was calculated by weighing two control coupons (clean and unexposed) before and after the cleaning according to the protocol ASTM G1-90 (1990) e1 (G01 Committee, 1999). The corrosion rate v_{corr} in mm/y was estimated using equation (1):

$$v_{corr} = (K.W)/(A.T.D) \quad \text{(equation 1)}$$

with K a constant (8.76×10^4), T the exposure time (h), A the coupon area (cm^2), W the weight loss (g), D is the density of the steel (g/cm^3).

Statistical analyses tests were also carried out to show significant differences between the estimated corrosion rates (Tukey's multiple comparisons test, CI = 95%, Prism-GraphPad).

2.6. Statistical analysis

In this paper, we used the corrplot package in RStudio to visualise and analyse the correlation matrix of our dataset. The corrplot function provides a versatile and visually appealing way to display correlation matrices, helping to identify patterns and relationships between variables (Friendly, 2002; Wei and Simko, 2010). A correlation matrix was realised confronting the following parameters (N = 148): immersion time, temperature (named *Temp* in the matrix), pH, redox potential (named *Redox*), salinity (*Sal*), dissolved oxygen concentration (*DO*), *Sargassum* presence (indices 0 for absence and 2 for presence), chromium content in steel composition (*Cr*) and corrosion rate (*Vcorr*).

2.7. Biofilm analysis

Prior to analysis, coupons were fixed according to the protocol above (see 2.4.2). Only 304L biofilm surfaces were observed by confocal laser scanning microscopy (CLSM) LSM 710, Zeiss®, as the black superficial

layers formed on the DC01 surface were easily removed and unstable. SS coupons were labelled in darkness using 100 μL of SYTO™ 9 (1 μM, Thermo Fisher Scientific®) and then covered with an 18 × 18 mm coverslip. After 15 min, images were captured by CLSM at 40x magnification (oil objective). Subsequently, two lasers were applied with 488 nm excitation in order to highlight the presence of DNA and a 633 nm excitation (emission: 500–550 nm and 650–700 nm respectively) was used for chlorophyll *a* (algae). CLSM was used on 220 × 220 μm zones and each 1 μm on the coupon to obtain 3D images. Biovolumes ($\mu m^3/\mu m^2$) were estimated using the COMSTAT program on MATLAB II software (Heydorn et al., 2000). Statistical tests were run to highlight differences between studied conditions (Mann-Whitney test, CI = 95%, Prism-GraphPad).

2.8. Bacterial analysis

2.8.1. Microbial community analysis

This analysis was only carried out on the 304L coupons as the DC01 coupons were too degraded by day 90 to be analysed. With the aim to determine the microbial community, biofilms were sampled on 304L coupons after 1 night, 7 days and 90 days of immersion, both from *Sargassum* thalli and from surrounding seawater at the same time. Coupons were rinsed with sterile tris buffered saline (TBS) to remove free living cells. Attached biofilm was scraped off in TBS using a sterile inoculator (Trigodet et al., 2019b). The biofilm in suspension was centrifuged at 4000 g, for 20 min at 4 °C to obtain a pellet. Before extraction, two thalli of *Sargassum* were rinsed with sterile TBS to remove free living bacteria, then biofilm was sampled from all zones (stipe, leaves) as described above. For seawater microbial analysis, 200 mL of water was filtered in duplicate on a 20 μm paper filter (Grosseron, France) to remove organic or inorganic matter, then filtered through a 0.2 μm biosart® membrane device (Sartorius®) (Trigodet et al., 2019a). One half of the membrane was used for biofilm inoculation and the other half for DNA extraction. DNA extraction was performed using the PowerLyzer PowerSoil Kit (Qiagen, France) (Smith et al., 2019) on pellets (304L SS and *Sargassum*) and on membrane filters (seawater) according to the manufacturer's recommendations. Quantification and quality of the total DNA were estimated by the ratio of absorbance at 260 and 280 nm using spectrophotometry (Vastra et al., 2016). Sequencing of the V3-V5 regions of 16S rRNA gene was carried out using the Illumina® Miseq® methods by Eurofins Genomics, Germany. Reads over 75% were used to obtain partial sequences which were processed using Cutadapt software to remove primers (Magoč and Salzberg, 2011). The FLASH algorithm was applied to contigs and chimaera were removed using UCHIME software. The method of minimum entropy decomposition method allowed the identification and classification of operational taxonomic units (OTUs) without requiring a 97% recovery of the sequences (Eren et al., 2015). Bacteria were grouped according to similarity. Sequence alignment was performed using DC-METABLAST software for a taxonomic assignment with over 70–80% of identification.

3. Results

3.1. Macro-degradations of steels and biofilm adhesion

The comparison of macrographs of DC01 and stainless steels at different times of immersion are displayed Fig. 1. At Co, black and orange corrosion product layers were present on the coupon surface of DC01. After 60 days of immersion at the Co site, macroscopic biofilms were observed on the coupon surface with attached macroalgae, which appeared to hold the corrosion products in place. At PM, thick, irregular and detachable layers of black corrosion products with some orange products increased over time when no macroscopic biofilms were visible. When, a comparison was done within *Sargassum* raft-exposed sites (PM and FE), for the same exposure duration, coupons from the FE site (fresh *Sargassum*) were less degraded, showing thin discontinuous black layers with visible unaltered steel layer, contrary to the PM site (decaying *Sargassum*). The most degraded DC01 coupons were from PM (Fig. 1A).

On the 304L SS (Fig. 1B), a thin gelatinous biofilm and organic matter were observed on day 7 on all sites. From day 60 to day 120, the biofilms were thicker on Co coupons with visible macroalgae. While, black corrosion products were present on the surface of coupons with pitting and aeration cells at PM, only an organic deposit with few barnacles was recorded on SS at FE. On day 7, on 304L coupons from all sites, bacterial microfouling was observed (Fig. 2). The biovolume was four times higher on coupons from the PM site (1.3 $\mu m^3/\mu m^2$) compared to those from Co (0.3 $\mu m^3/\mu m^2$) but their difference was statistically insignificant (p-value >0.05) (Fig. 2). In contrast, a significant difference was revealed when the biovolume of coupons from PM and FE (0.1 $\mu m^3/\mu m^2$) was compared. On day 60, an increase in microfouling composed of bacteria and microalgae (red) was observed on coupons immersed at Co and FE compared to PM. However, on day 60, biovolume estimation was not relevant because of the thickness of the biofilm.

3.2. Influence of Sargassum on corrosion rates

Corrosion rates were estimated using the mass loss measurement method and then compared with the classes of corrosion rates listed in the standard NACE RP-0775-2005 (NACE, 2005). Each class is associated with a level of corrosion severity: low (<0.025 mm/year), moderate (between 0.025 and 0.125 mm/y), high (between 0.126 and 0.254 mm/y) and severe (>0.254 mm/y).

Fig. 3A shows that the highest corrosion rate obtained with DC01 was 9.0 ± 0.01 mm/y at PM compared to Co (1.4 ± 0.01 mm/y). Both correspond to severe corrosion following the NACE Standard. However, significant differences in corrosion rates at PM were observed between day 0 and day 7 (p-value >0.001) and on day 7 with Co coupons (p-value >0.01). At both sites, an increase from day 0 to day 7, then a drop from day 7 to day 15 of the corrosion rate were observed. After day 15, a steady decline was measured for PM, while a slight raise was recorded for Co. This decrease between day 7 and day 15 could be explained by an increase in the thickness of the layers of corrosion products limiting the diffusion of O_2 towards the internal interface of the oxidised samples (Palanichamy et al., 2012).

In the case of 304L (Fig. 3B), the most important corrosion rate was also recorded at PM. The higher corrosion rate was 0.1 ± 0.02 mm/y at PM compared to 0.02 ± 0.01 mm/y for Co on day 90. Highly significant differences were found between day 0 and day 90 at PM (p-value <0.0001), between PM and Co coupons at day 90 (p-value <0.001) and between day 0 and at both sites coupons at day 120 (p-value <0.001). Variations in v_{corr} at PM with alternating increases and slight decreases compared to Co was noted. Furthermore, according to the NACE standard, on the PM site, the level of corrosion recorded corresponds to a moderate level while that obtained on the Co site belongs to the low class.

3.3. Influence of Sargassum on physicochemical parameters of seawater

As shown in Fig. 4, significant low pH (6.5 ± 0.1), redox potential (−299 ± 7.9 mV/Ag/AgCl) and DO (1.7 ± 0.8 mg/L) have been recorded for PM (decaying alga) in comparison to Co (absence or low alga; pH: 7.8 ± 0.1), redox potential: 46 ± 4 mV/Ag/AgCl) and DO: 4.9 ± 1.7 mg/L) respectively. But, no significant variations were observed for temperature and salinity (Fig. S2).

PM seawater illustrated a reductive and anoxic environment and Co was an oxidative and oxic environment. However, during episodic massive *Sargassum* strandings (only leachates remained), the DO concentration recorded at Co was similar to that observed at PM. In comparison with FE (fresh *Sargassum* condition), the pH was 7.3 ± 0.02, the

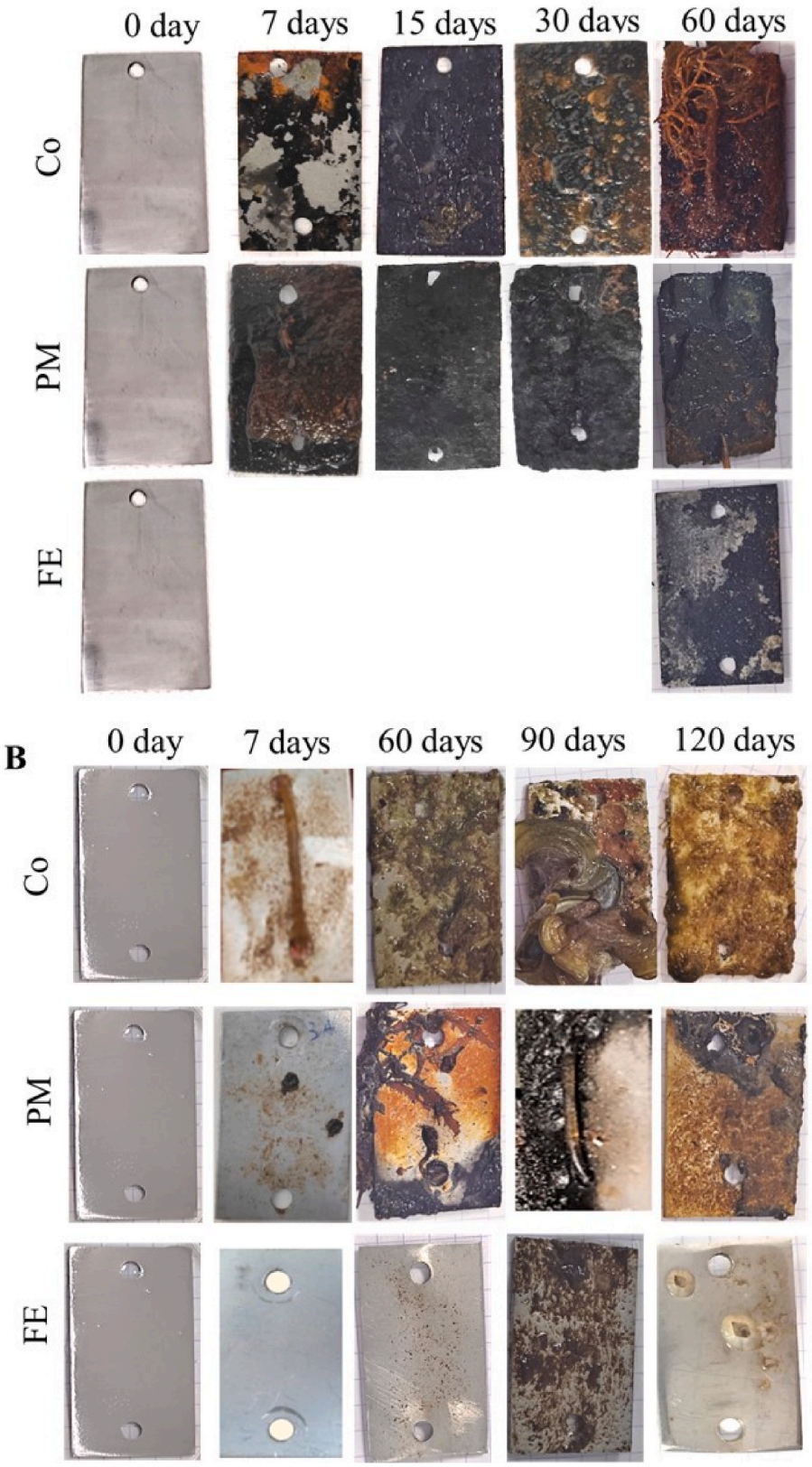

Fig. 1. A - Macrophotographs of carbon steel DC01 at 0, 7, 15, 30 and 60 days of immersion in seawater at Port of Marigot (PM), Frégate Est 2 (FE2) and Cosmy bay (Co). B - Macrophotographs of stainless steel 304L at 0, 7, 60, 90, 120 days' immersion in seawater at Port of Marigot (PM), Frégate Est 2 (FE) and Cosmy bay (Co).

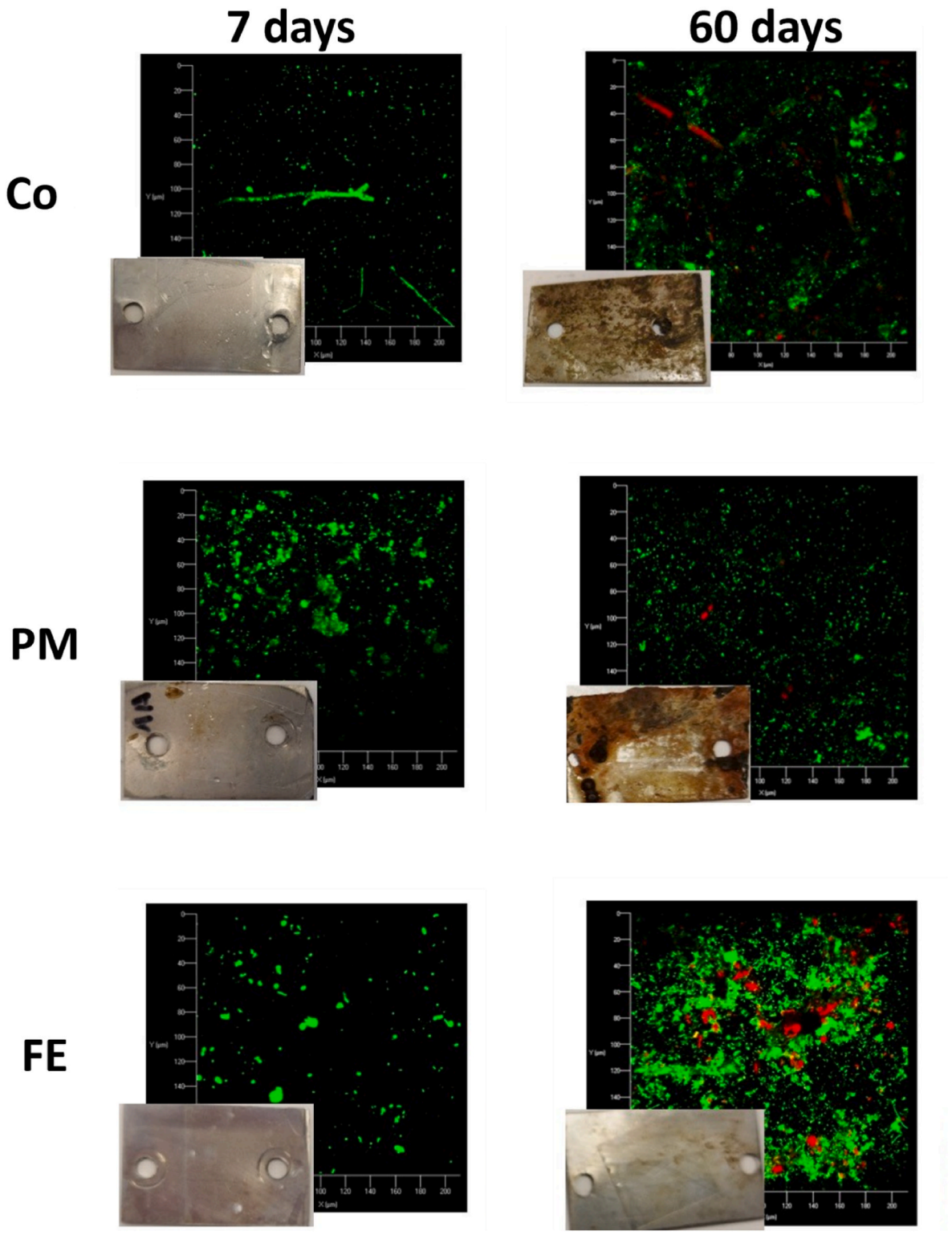

Fig. 2. Confocal laser scanning microscopy (CLSM) images of SS 304L surfaces after 7 days and 60 days of immersion in seawater for Co, PM and FE.

redox potential was −106 ± 17 mV/Ag/AgCl) and the DO concentration was 2.7 ± 0.4 mg/L. All of our results suggested a negative relationship between pH, DO, redox and the presence of Sargassum.

Moreover, Pearson's correlation matrix (Fig. S3) showed a high positive correlation coefficient between physicochemical parameters as follows: pH and redox (0.85), pH and DO (0.82), DO and redox (0.70), indicating a positive correlation and proportionality between these parameters. Furthermore, a significant negative correlation coefficient was observed between the presence of *Sargassum* and pH (−0.81), *Sargassum* and Redox (−0.61), and *Sargassum* and DO (−0.68), confirming the negative influence of the presence of *Sargassum* on pH, DO, and redox observed in our study. However, the correlation between *Sargassum* presence and corrosion rate (v_{corr}) was weaker (0.33).

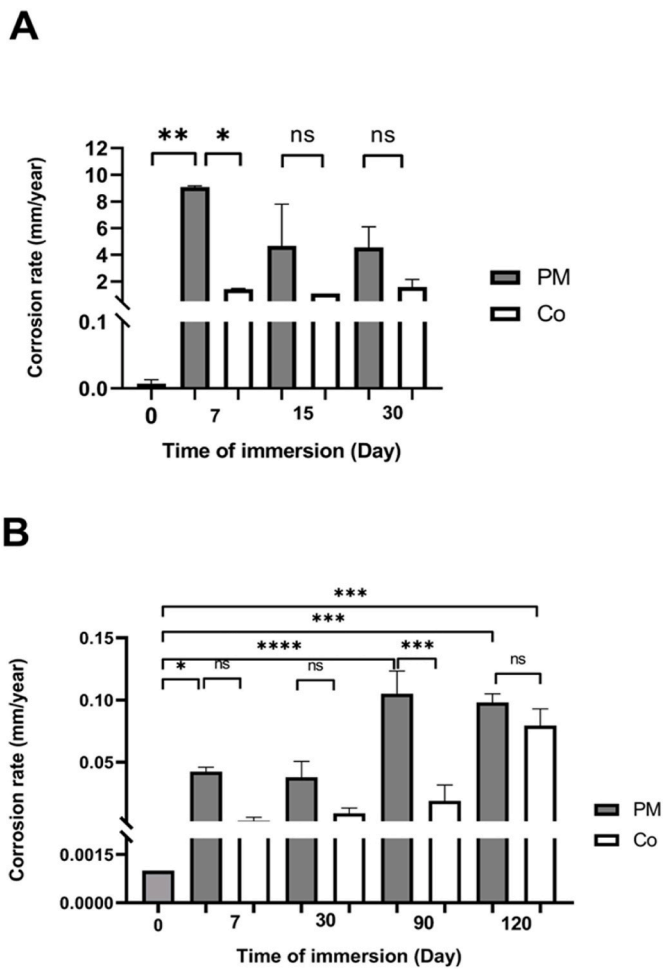

Fig. 3. A-Corrosion rate calculated from mass loss of coupons exposed in seawater from 0, 7, 15, 30 days at Port of Marigot (PM) and Cosmy (Co) for DC01 with standard deviation except for Co at 15d. Significant differences calculated with Tukey multiple comparison test: ns p-value >0.05; *p-value <0.01; **p-value >0.001. B - Corrosion rate calculated from mass loss of coupons exposed in seawater from 0, 7, 60, 90, 120 days at Port of Marigot (PM) and Cosmy (Co) for 304L with standard deviation Significant differences calculated with Tukey multiple comparison test: ns p-value >0.05; *p-value >0.01; **p-value >0.001; ***p-value <0.001; ****p-value <0.0001.

3.4. Surface analysis of immersed steel coupons

3.4.1. Chemical composition of corrosion deposit

The SEM-EDS analysis focused on DC01 coupons (Fig. S4), which exhibited a high accumulation of corrosion products compared to other steel, on day 7 and day 60. Iron (in blue) and oxygen (in green) were observed on the surface of corroded coupons for all sites. Generally, these elements are found in corrosion products layers in aerated medium (Fig. S4A). However, sulphur was only detected on PM and FE coupons suggesting that its presence was correlated with high alga density.

XRD spectra analysis on DC01 coupons of the PM and Co sites highlighted the presence of magnetite, goethite, lepidocrocite and akaganeite in all coupons on day 10 of immersion (Fig. 5). Additionally, elemental sulphur was only detected on the PM's coupons. However, on day 30, lepidocrocite was absent and sulphur remained present on PM compared to Co, where no variations in the composition over time were observed. But, no ferrous sulphides were detected on PM's coupons. On 316L, iron, sodium chloride and silicon dioxide were common products found. Elemental sulphur was also present at PM coupons on day 30 of immersion, whereas magnetite was only identified on Co coupons.

3.5. Microbial communities

3.5.1. Implication of bacterial composition

The microbial diversity of 304L coupon biofilms, collected after 90 days of immersion from PM and Co sites, along PM's seawater and *Sargassum* samples from the PM site, were evaluated through analysis of the 16S rRNA gene (Fig. 6). At the class level, sequence analysis depicted a higher diversity of OTU in bacterial communities within all conditions of the PM site. In fact, five classes were identified on Co coupons which were dominated by *Alphaproteobacteria* (89%), *Flavobacteriia* (8%) compared to up to seven classes found in PM site conditions (Fig. 6). In 304L SS biofilms (PM), *Alphaproteobacteria* (72%) was also the most dominant class, followed by *Desulfuromonadia* (7%), *Desulfobulbia* (6%).

A difference between coupons, planktonic and *Sargassum* microbiomes at the PM site was observed. In the planktonic community, *Epsilonproteobacteria* (38%) was dominant, followed by *Spirochaetia* (12%), *Clostridia* (12%) *and Alphaproteobacteria* (11%), *Desulfuromonadia* (10%). In *Sargassum* biofilm, *Desulfuromonadia (*27%) and *Desulfobulbia* (26%) were the most abundant followed by *Spirochaetia* (15%), *Desulfobacteria* (9%), *Flavobacteriia* (6%), *Clostridia* (6%), *Bacteroidia* (4%), *Desulfovibrionia* (2%). Thus, bacteria with a sulphate respiration (*Desulfobulbia*, *Desulforomonadia*) belonging to SRB group have been found both in *Sargassum* biofilm and 304L SS biofilm at PM whereas none have been presented at Co.

At species level (Fig. S5), microbial diversity was lower on the PM 304L coupon in comparison to those of Co, with a dominance of species belonging to *Thioclava* (49%) and *Rhodobacteraceae* family (14%). In PM seawater, *Arcobacter venerupis* (36%) and *Petrocella atlantisensis* (12%) were more abundant, whereas the most abundant species in *Sargassum* biofilm were *Pelobacter* sp. (26%) and *Desulfobacter latus* (19%). Also, species such as *P. atlantisensis* were found in all samples of PM, *Desulforhopalus* sp. which is a strict anaerobe, majorly can reduce sulphate and fermentation (Galushko and Kuever, 2019) was present in *Sargassum* (19%) and 304L SS (4.6%) biofilm at PM. Also, *Desulfobulbus rhabdoformis*, a sulphate-reducing bacteria known in biocorrosion (Lien et al., 1998), was identified only in 304L biofilm (0,1%) at PM. In addition, SRB, which are anaerobes, as *Pelobacter* sp., *Desulfovibrio* sp., *Desulfobulbus* sp. were mostly detected in *Sargassum* biofilms.

4. Discussion

In the literature, average corrosion rates in seawater are estimated for CS between 0.13 mm/y after several years of exposition (Al-Fozan and Malik, 2008) to 1 mm/y when exposed in an accelerated low-water corrosion (ALWC) area (Smith et al., 2019). In the case of SS, the corrosion rate is about 0.014 mm/y for 304L SS in fully immersed conditions (Arroussi et al., 2022). In the study presented here, the *Sargassum*-free site Co showed corrosion rates equivalent to these values, while the PM site, with a high density of decayed Sargassum, showed corrosion rates 9 times higher for CS (9.0 mm/y) and 10 times higher for 304L SS (0.1 mm/y). These first observations validate the selection of sites for our study. In fact, although all the sites had similar features in terms of currentology, urbanisation and wave protection (bays, seawalls or coral reefs), Co presented the classic characteristics of seawater, while PM displayed exceptional aggressiveness towards exposed materials. Between the two, FE enabled us to identify the role of the algae's state of degradation on the results, particularly in terms of erosion speed and products.

Thus, the Co site was characterised by physicochemical values within the known normals for seawater. Under these conditions, the corrosion mechanisms generally described are those due to the combined are controlled by the action of chloride ions and dissolved oxygen (Bhandari et al., 2015; Pusparizkita et al., 2023). As for the PM site, it showed a degraded physicochemical state, certainly related to the high density of *Sargassum* present in the water column of only a few tens of centimetres. Indeed, pH values recorded at the site were below literature and control

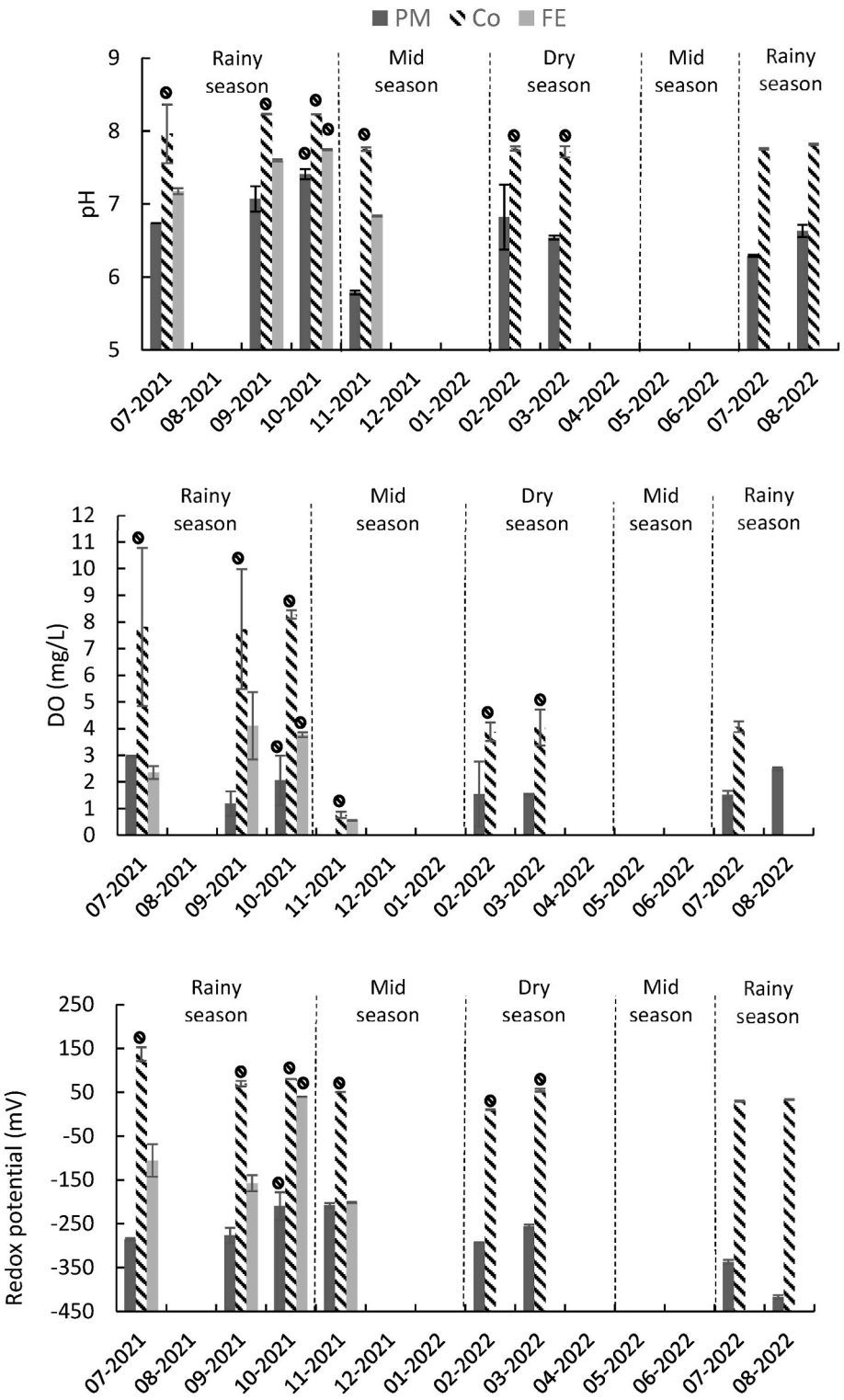

Fig. 4. Mean values of physico-chemical parameters (pH, DO, redox) monitored over study period with standard deviation. markers indicate absence of *Sargassum* strandings *in situ*.

values, as were OD and redox potential. Although oxygen-poor seawater inhibits diffusion-controlled corrosion, corrosion processes driven by the chloride ions, H_2S and the metabolism bacteria such as SRB are favoured (Phull, 2010; Valdez et al., 2016).

The decrease in pH at PM could be explained by the important decomposition of *Sargassum* releasing acid compounds such as hydrogen sulphide, lactic acid and CO_2 (Antonio-Martínez et al., 2020; Rodríguez-Martínez et al., 2019). The degradation of algae could be indirectly assessed by the average concentration of H_2S of 5 ± 3 ppm in the vicinity of the coupons. Apart from being corrosive, high soluble H_2S coupled with elevated CO_2 concentrations have been shown to cause a drop in the pH (Choi et al., 2011; Ruiz-Luna et al., 2019). Also, the variations of corrosion rates of 304L SS observed at PM over time could correspond to cycles of passive film formation and breakdown caused by

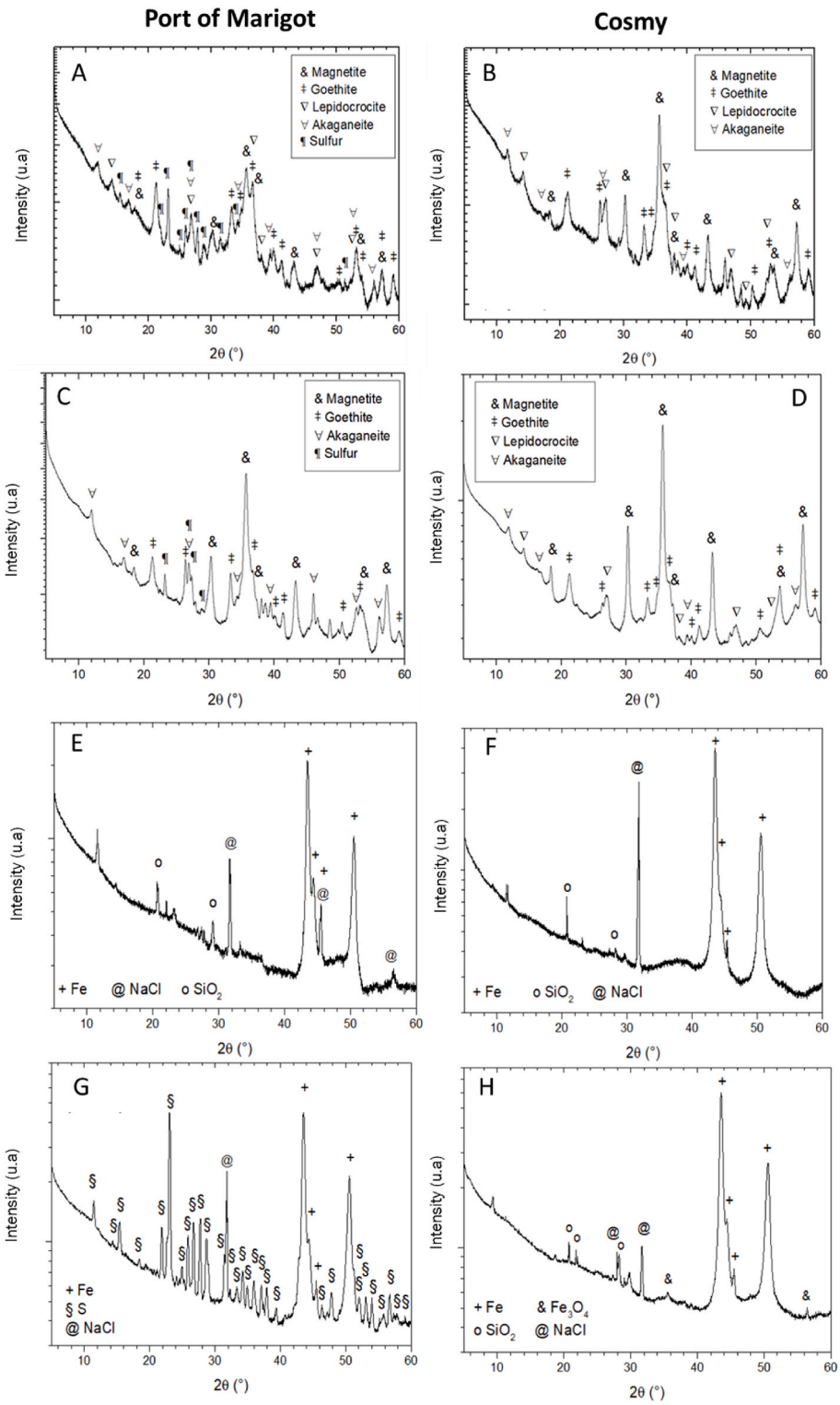

Fig. 5. DRX spectra coupons immersed at Port of Marigot (A–G) and at Cosmy (B–H) for 10 days (A, C) and 30 days (B, D) for DC01 and 10 days (E, G) and 30 days (F–H) for 316L.

the presence of corrosive species such as H_2S (Chen et al., 2017; Li et al., 2014). Hydrogen sulphide is a reducing acid in solution known to increase the rate of oxygen reduction, and subsequently decrease in the redox potential (Wiener et al., 2006; Yin and Wu, 2016). Interestingly, our study highlighted for the first time its co-presence with decaying *Sargassum*.

In addition, the formation of corrosion products is influenced by physicochemical parameters such as pH and DO (Kooli et al., 2018). The variation of these parameters between the three sites explain the difference of corrosion by-products on the coupon surfaces. In seawater, corrosion products formed a rust composed of three layers: outer (red-brown), middle (orange) and inner (black) layers. Orange and brown corrosion products often compose outer layers in presence of oxygen. It corresponded to iron oxides, hydroxides or oxyhydroxides as

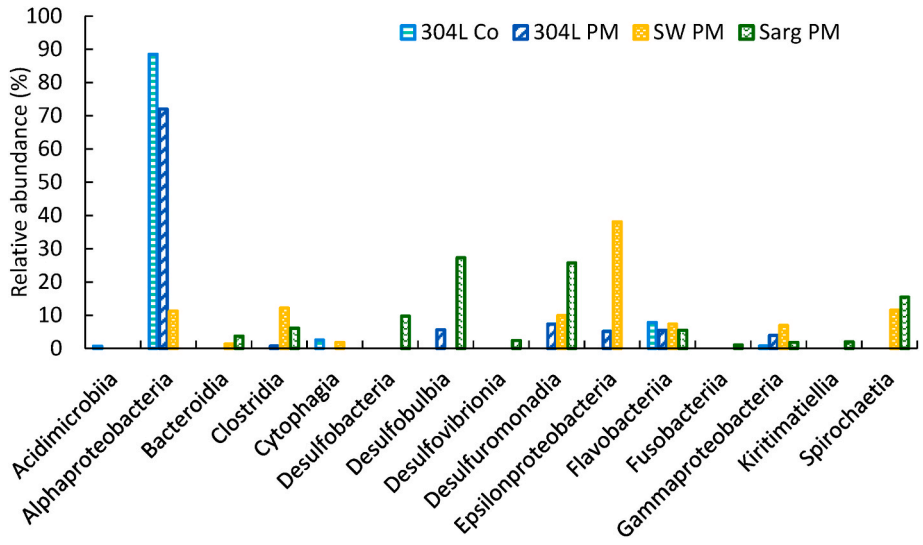

Fig. 6. Relative abundance of bacterial communities (at class level): in biofilm harvested from 304L immersed at Cosmy (A), in biofilm harvested from 304L immersed at Port of Marigot (B), in seawater of Port of Marigot (C) and in biofilm harvested from *Sargassum* leaves at Port of Marigot (D).

lepidocrocite (Pusparizkita et al., 2023), goethite. Whereas, black products are in inner layers near metal as magnetite (Pineau et al., 2008), as seen at Cosmy site. For example, lepidocrocite is porous, formed in the presence of a flow of oxygen at the early stage of the corrosion. In contrast, magnetite is formed in a compact layer in O_2-depleted zones, where anaerobes bacteria grow (Lanneluc et al., 2015; Mercier-Bion et al., 2016), from restricted oxidation of ferric hydroxides or reduction of lepidocrocite. It could be formed more easily with reductive conditions as reported above for PM with low DO and negative redox potential.

Moreover, the presence of H_2S, from decomposition of algae, could imply a mechanism similar to corrosion of the metal in neutral sulphide abiotic environment (pH 6–13) including: i) chemical absorption of H_2S leading to chemisorption reactions and electronic discharges in the anodic zone, resulting in the formation of sulphides such as mackinawite (equation (2)) and ii) reduction of H_2S (equation (3)) (Marchal, 1999).

$$Fe_{(s)} + H_2S_{(g)} + H_2O_{(l)} \rightarrow FeSH^-_{ads} + H_3O^+_{(aq)} \quad \text{(equation 2)}$$

$$2H_2S_{(g)} + 2e^- \rightarrow H_{2(g)} + 2HS^-_{(aq)} \quad \text{(equation 3)}$$

In this condition, corrosion of mild steel such as DC01, in a liquid medium saturated with H_2S, is uniform. This dissolved gas is a weak acid that could be formed by bisulphide (HS^-) and sulphide (S^{2-}) in seawater by ionic dissociation (Wiener et al., 2006) or react with iron from coupons forming some iron sulphides (equation (4)):

$$Fe_{(s)} + H_2S_{(g)} = FeS_{(s)} + H_{2(g)} \quad \text{(equation 4)}$$

Then, this reaction allows the formation of sulphide-rich forms such as mackinawite, iron sulphides and pyrite composing corrosion products (Cifuentes et al., 2020) and also facilitating the reductive dissolution of the iron oxides layer of SS (Keresztes et al., 2001). In biotic conditions, H_2S is also produced by SRB metabolism by sulphate reduction (Guezennec, 1990; Usher et al., 2014). Sulphates as an electron acceptor is reduced to produce sulphide compounds in anaerobic conditions in biofilms using iron as the electron donor (Enning and Garrelfs, 2014) and forming iron sulphides. These products could be oxidised giving products as iron oxyhydroxides, sulphates and acid sulphuric attacking the steel (Refait et al., 2013).

In our study, no iron sulphides were detected in the corrosion products whereas sulphur was detectable under its elemental form for PM and FE exposed coupons. This absence could be in reality due to an amorphous form non visible by XRD (Said Ahmed et al., 2024). However, two mechanisms could explain the presence of elemental sulphur. First, at high tide, with low oxygen, the role of SRB and SOB induce accelerated corrosion (Little and Lee, 2007). Sulphur-oxidising bacteria (SOB) such as *Thiobacillus* genus or filamentous species as *Beggiatoa* normally produce oxidised sulphur compounds from H_2S produced by SRB (Brock and Gustafson, 1976; Little and Lee, 2007) such as elemental sulphur (Kabil et al., 2014) or thiosulphates (Mercier-Bion et al., 2016; Pineau et al., 2008; Wakai et al., 2022). At low tide and in aerated conditions, the formation of elemental sulphur could depend on the reaction of H_2S and organic matter (Cifuentes et al., 2020).

Biofilm formation on steel surfaces could lead to various issues, such as metal corrosion linked in particular to microbial metabolism (Dang and Lovell, 2016). In order to understand their role, an analysis of bacterial communities has been carried out. Massive green tides have been reported to release sulphur compounds (Wan et al., 2017). Also, these tides, during the degradation, create anaerobic conditions favourable for the growth of SRB (Qu et al., 2020). This phenomenon could be comparable to what it was observed on the Martinique coasts. The differences observed between Co 304L SS biofilm (presence of macroalga, organic matter), FE 304L SS biofilm (barnacles, organic matter) and PM 304L SS biofilm (organic deposit, decaying alga) could be link to physicochemical parameters variations and H_2S. A decrease in pH could affect the stability of macromolecules and could cause the denaturation of proteins, affecting biological mechanisms and biofilm establishment (Koschorreck, 2008). Whereas, an O_2 concentration from 0.28 mg/L to 4 mg/L reduces the diversity of species present in the medium (Mukherjee et al., 2013; Vaquer-Sunyer and Duarte, 2008) as seen with the absence of macroscopic biofilm at PM. Moreover, the presence of barnacles indicated that the physicochemical parameters were different at FE. Barnacles are the most common and resilient macrofouling organisms, which can permanently attach to solid structures in seawater with cement proteins causing localised corrosion at fouling attachment by metal dissolution (Murugan et al., 2020). Moreover, these organisms are known to be environmental changes' bio-indicators, in particular for variations of pH and DO in seawater (Chen et al., 2014). In fact, pH of 7.6 coupled to DO of 3 mg/L decrease the settlement of larvae on solid surface. In addition, barnacles are more sensitive to hypoxia (Campanati et al., 2016).

Indeed, in *Sargassum* biofilm, 3.8% of identified OTU of prokaryotes use sulphur compounds for respiration (Hervé et al., 2021). In our study, most of the sulfidogenic anaerobes bacteria with a sulphate reducing metabolism belonging to *Desulfuromonodia, Desulfobulbia, Desulfovribrionia* or *Desulfobacteria* were found at PM on sargassum and on coupon

biofilms. SRB such as *Desulfovibrionaceae* but also *Spirochaetaceae* play a major role in sulphur biogeochemical cycling. SRBs are considered as the main culprit of MIC in anoxic environments (Little and Lee, 2007; Wang et al., 2023; Y. and Mulky, 2023). In anaerobic biocorrosion, two mechanisms realised by microorganisms are described: i) an attack by extracellular transfer induce by respiration, as SRB with sulphate reduction, ii) an attack by metabolite with the production of corrosive products with the secretion of acids secreted by APB (Gu et al., 2021; Herrera and Videla, 2009; Li et al., 2017; Little et al., 2020; Vigneron et al., 2016). The first corresponds to a direct attack of the metal by oxidation of the steel allowing an electron uptake. This oxidation can occur in the presence of potential depolarising agents such as sulphate and nitrate. There are two types of extracellular electron transfer (EET): i) a direct electron transfer (DET) which involves the transport of electrons through the microbial cell wall by membrane proteins such as c-type cytochromes (Beech and Sunner, 2004) or conductive pili (Usher et al., 2014) to an intracellular hydrogenase-mediated electron transfer system (Duan et al., 2008; Gu et al., 2021). In this mechanism, bacteria, such as *Desulfovibrio vulgaris*, are in contact with the metal to use this pathway for respiration; ii) a mediated electron transfer (MET) which implies the presence of soluble electron transfer mediators (Lu et al., 2024b). These mediators are responsible for transporting of electrons from the metal (Fe^0) to the microbial cell membranes (Jia et al., 2017). The carriers, as H^+/H_2 and flavins (flavin adenine dinucleotide (FAD) and riboflavin), have redox activities (Lu et al., 2024a). The redox shuttles, in their oxidised form, absorb the electrons and then release them to the membranes, in their reduced form. In this way, the bacteria in the biofilm that are not in contact with the steel can also increase the EET.

Bacteria such as SRB can use iron as an electron donor for energy production in sulphate respiration (Enning et al., 2012). These electroactive bacteria can catalyse oxidation and reduction reactions in biofilm. Thus, the biofilm formed on the steel surface is electrogenic and accelerates MIC (Liu et al., 2015).

The second implies metabolic by-products. Among these bacteria, some can also use CO_2 or organic matter/carbon as energy sources in micro-aerobic and anaerobic environments (Emerson, 2018). From decomposition of organic matter, SRB can also produce H_2 that can diffuse in the metal causing cracking and brittle fracture in the steel (Li et al., 2024). This corrosion phenomenon is known as stress cracking corrosion (SCC).

Rhodobacterales (*Thioclava* sp., *Maritimibacter lacisalsi*), presented in 304L SS biofilm, are also known to cause pitting corrosion (De La Fuente et al., 2020). Others bacteria such as *Gammaproteobacteria* (as *Alteromonas* sp.) are considered to be the first colonisers of immersed surfaces in early stages of biofilm formation (Ma et al., 2020) and have a good resistance to environmental variations (Dennis Enning et al., 2012), *Spirochaetota, Bacteroidia* and *Bacillota* has an ability to degrade organic matter and could grow in hypoxic environments (Chen et al., 2020; Köchling et al., 2015); these conditions could be in favour of the development of SRB. MIC implies organisms which are physiologically different forming a consortium distributed in biofilm on the surface of the steel (Černoušek et al., 2020; Li et al., 2020; Y. and Mulky, 2023).

5. Conclusion

Our work demonstrated for the first time that i) macroalgae *Sargassum* strandings, in particular when they are in highly degraded state, have a negative impact on the physicochemical and biological state of seawater, ii) within high density decomposed alga rafts, corrosion of immersed steel is severe and shows exceptional high values of rate. All data recorded for 2 years from our experimental sites, one heavily exposed to sargassum tides with decomposing alga and another few exposed to macroalgae tides, provided key data. We highlighted that the decaying *Sargassum* lowers the pH, creates an anoxic and reductive environment in coastal zones. Moreover, anaerobic conditions favour the growth of sulphate-reducing bacteria (SRB) in the coupon surface biofilm. Their implication in the corrosion process is remarkable with the presence of sulphur in the corrosion product layers. Those results confirm the urgency for those involved in the public sectors to collect the seaweed as quickly as possible, to protect the coastal population and to limit metallic structures degradation.

CRediT authorship contribution statement

Diana Bénuffé: Writing – original draft, Methodology, Investigation, Conceptualization. **Fatima Radouani:** Writing – original draft, Methodology, Investigation, Conceptualization. **Maxence Quemener:** Methodology. **Olivia Ozier:** Investigation. **Marilyne Fauchon:** Methodology, Investigation. **Yannick Toueix:** Investigation. **Fabienne Faÿ:** Investigation, Formal analysis, Conceptualization. **Anthony Magueresse:** Investigation. **Benoit Lescop:** Writing – review & editing, Investigation, Conceptualization. **Stéphane Rioual:** Writing – review & editing, Investigation, Conceptualization. **Pascal Zongo:** Writing – review & editing, Formal analysis. **Christophe Roos:** Validation, Supervision, Methodology, Funding acquisition, Conceptualization. **Claire Hellio:** Writing – review & editing, Validation, Supervision, Methodology, Conceptualization. **Paule Salvin:** Writing – original draft, Validation, Supervision, Project administration, Methodology, Funding acquisition, Conceptualization.

Declaration of competing interest

The authors declare that they have no known competing financial interests or personal relationships that could have appeared to influence the work reported in this paper.

Acknowledgement

This work was supported by the French National Research Agency [ANR 19 SARG 0006]; Collectivité Territoriale de Martinique and European Regional Development Fund [PO FEDER MQ0027404].

Appendix A. Supplementary data

Supplementary data to this article can be found online at https://doi.org/10.1016/j.marenvres.2024.106924.

Data availability

Data will be made available on request.

References

Al-Fozan, S.A., Malik, A.U., 2008. Effect of seawater level on corrosion behavior of different alloys. Desalination 228, 61–67. https://doi.org/10.1016/j.desal.2007.08.007.

Antonio-Martínez, F., Henaut, Y., Vega-Zepeda, A., Cerón-Flores, A.I., Raigoza-Figueras, R., Cetz-Navarro, N.P., Espinoza-Avalos, J., 2020. Leachate effects of pelagic Sargassum spp. on larval swimming behavior of the coral Acropora palmata. Sci. Rep. 10, 3910. https://doi.org/10.1038/s41598-020-60864-z.

Antunes, J., Leão, P., Vasconcelos, V., 2019. Marine biofilms: diversity of communities and of chemical cues. Environ. Microbiol. Rep. 11, 287–305. https://doi.org/10.1111/1758-2229.12694.

Arroussi, M., Jia, Q., Bai, C., Zhang, S., Zhao, J., Xia, Z., Zhang, Z., Yang, K., Yang, R., 2022. Inhibition effect on microbiologically influenced corrosion of Ti-6Al-4V-5Cu alloy against marine bacterium Pseudomonas aeruginosa. J. Mater. Sci. Technol. 109, 282–296. https://doi.org/10.1016/j.jmst.2021.08.084.

Bates, N.R., Johnson, R.J., 2020. Acceleration of ocean warming, salinification, deoxygenation and acidification in the surface subtropical North Atlantic Ocean. Commun. Earth Environ. 1, 1–12. https://doi.org/10.1038/s43247-020-00030-5.

Beech, I.B., Sunner, J., 2004. Biocorrosion: towards understanding interactions between biofilms and metals. Curr. Opin. Biotechnol. 15, 181–186. https://doi.org/10.1016/j.copbio.2004.05.001.

Benaïssa, B., 2004. La corrosion des structures métalliques en mer : types et zones de dégradations, in: VIIIèmes Journées, Compiègne. Present. Journées Nationales Génie

Côtier - Génie Civil, Editions Paralia 667–677. https://doi.org/10.5150/jngcgc.2004.074-B.
Bermont-Bouis, D., Janvier, M., Grimont, P.a.D., Dupont, I., Vallaeys, T., 2007. Both sulfate-reducing bacteria and Enterobacteriaceae take part in marine biocorrosion of carbon steel. J. Appl. Microbiol. 102, 161–168. https://doi.org/10.1111/j.1365-2672.2006.03053.x.
Bhandari, J., Khan, F., Abbassi, R., Garaniya, V., Ojeda, R., 2015. Modelling of pitting corrosion in marine and offshore steel structures – a technical review. J. Loss Prev. Process. Ind. 37, 39–62. https://doi.org/10.1016/j.jlp.2015.06.008.
Boudaud, N., Pineau, S., Amiel, C., 2010. Characterization of microbial flora associated with marine corrosion: the contribution of FT-IR spectroscopy. Matériaux Tech. 98, 69–79. https://doi.org/10.1051/mattech/2010013.
Brock, T.D., Gustafson, J., 1976. Ferric iron reduction by sulfur- and iron-oxidizing bacteria. Appl. Environ. Microbiol. 32, 567–571. https://doi.org/10.1128/AEM.32.4.567-571.1976.
Brooks, M.T., Coles, V., Hood, R., Gower, J., 2018. Factors controlling the seasonal distribution of pelagic Sargassum. Mar. Ecol. Prog. Ser. 599, 1–18. https://doi.org/10.3354/meps12646.
Bunet, R., 2020. Biofouling et antifouling biologique. In: L'agriculture Durable, pp. 293–312.
Butko, D., Vilson, E., Yakovleva, E., 2017. The use of a redox indicator to determine corrosiveness of wastewater towards metal structures. MATEC Web Conf. 106, 07003. https://doi.org/10.1051/matecconf/201710607003.
Cabanillas-Terán, N., Hernández-Arana, H.A., Ruiz-Zárate, M.-Á., Vega-Zepeda, A., Sanchez-Gonzalez, A., 2019. *Sargassum* blooms in the Caribbean alter the trophic structure of the sea urchin *Diadema antillarum*. PeerJ 7, e7589. https://doi.org/10.7717/peerj.7589.
Campanati, C., Yip, S., Lane, A., Thiyagarajan, V., 2016. Combined effects of low pH and low oxygen on the early-life stages of the barnacle Balanus amphitrite. ICES (Int. Counc. Explor. Sea) J. Mar. Sci. 73, 791–802. https://doi.org/10.1093/icesjms/fsv221.
Campbell, S.A., Beech, I.B., 2009. Accelerated low water corrosion: causes and consequences. In: Presented at the 49th Annual Conference of the Australasian Corrosion Association 2009: Corrosion and Prevention 2009, pp. 40–49.
Černoušek, T., Shrestha, R., Kovářová, H., Špánek, R., Ševců, A., Sihelská, K., Kokinda, J., Stoulil, J., Steinová, J., 2020. Microbially influenced corrosion of carbon steel in the presence of anaerobic sulphate-reducing bacteria. Corrosion Eng. Sci. Technol. 55, 127–137. https://doi.org/10.1080/1478422X.2019.1700642.
Chen, J., Li, H., Zhang, Z., He, C., Shi, Q., Jiao, N., Zhang, Y., 2020. DOC dynamics and bacterial community succession during long-term degradation of Ulva prolifera and their implications for the legacy effect of green tides on refractory DOC pool in seawater. Water Res. 185, 116268. https://doi.org/10.1016/j.watres.2020.116268.
Chen, S., Frank Cheng, Y., Voordouw, G., 2017. A comparative study of corrosion of 316L stainless steel in biotic and abiotic sulfide environments. Int. Biodeterior. Biodegrad. 120, 91–96. https://doi.org/10.1016/j.ibiod.2017.02.014.
Chen, Z.-F., Zhang, H., Wang, H., Matsumura, K., Wong, Y.H., Ravasi, T., Qian, P.-Y., 2014. Quantitative proteomics study of larval settlement in the barnacle Balanus amphitrite. PLoS One 9, e88744. https://doi.org/10.1371/journal.pone.0088744.
Choi, Y.-S., Nesic, S., Ling, S., 2011. Effect of H2S on the CO2 corrosion of carbon steel in acidic solutions. Electrochim. Acta 56, 1752–1760. https://doi.org/10.1016/j.electacta.2010.08.049.
Cifuentes, G.R., Jiménez-Millán, J., Quevedo, C.P., Jiménez-Espinosa, R., 2020. Transformation of S-bearing minerals in organic matter-rich sediments from a saline lake with hydrothermal inputs. Minerals 10, 525. https://doi.org/10.3390/min10060525.
Creus, J., Sabot, R., Refait, P., 2004. Corrosion et protection des métaux en milieu marin. Bioprocédés et bioproductions. https://doi.org/10.51257/a-v1-cor620.
Daille, L.K., Aguirre, J., Fischer, D., Galarce, C., Armijo, F., Pizarro, G.E., Walczak, M., De la Iglesia, R., Vargas, I.T., 2020. Effect of tidal cycles on bacterial biofilm formation and biocorrosion of stainless steel AISI 316L. J. Mar. Sci. Eng. 8, 124. https://doi.org/10.3390/jmse8020124.
Dang, H., Lovell, C.R., 2016. Microbial surface colonization and biofilm development in marine environments. Microbiol. Mol. Biol. Rev. 80, 91–138. https://doi.org/10.1128/MMBR.00037-15.
De La Fuente, M.J., Daille, L.K., De la Iglesia, R., Walczak, M., Armijo, F., Pizarro, G.E., Vargas, I.T., 2020. Electrochemical bacterial enrichment from natural seawater and its implications in biocorrosion of stainless-steel electrodes. Materials 13. https://doi.org/10.3390/ma13102327.
Duan, J., Wu, S., Zhang, X., Huang, G., Du, M., Hou, B., 2008. Corrosion of carbon steel influenced by anaerobic biofilm in natural seawater. Electrochim. Acta 54, 22–28. https://doi.org/10.1016/j.electacta.2008.04.085.
Dvoracek, L.M., 2013. Pitting corrosion of steel in H2S solutions. Corrosion 32, 64–68. https://doi.org/10.5006/0010-9312-32.2.64.
Emerson, D., 2018. The role of iron-oxidizing bacteria in biocorrosion: a review. Biofouling 34, 989–1000. https://doi.org/10.1080/08927014.2018.1526281.
Enning, D., Garrelfs, J., 2014. Corrosion of iron by sulfate-reducing bacteria: new views of an old problem. Appl. Environ. Microbiol. 80, 1226–1236. https://doi.org/10.1128/AEM.02848-13.
Enning, D., Venzlaff, H., Garrelfs, J., Dinh, H.T., Meyer, V., Mayrhofer, K., Hassel, A.W., Stratmann, M., Widdel, F., 2012. Marine sulfate-reducing bacteria cause serious corrosion of iron under electroconductive biogenic mineral crust: microbial iron corrosion under electroconductive crust. Environ. Microbiol. 14, 1772–1787. https://doi.org/10.1111/j.1462-2920.2012.02778.x.
Eren, A.M., Morrison, H.G., Lescault, P.J., Reveillaud, J., Vineis, J.H., Sogin, M.L., 2015. Minimum entropy decomposition: unsupervised oligotyping for sensitive partitioning of high-throughput marker gene sequences. ISME J. 9, 968–979. https://doi.org/10.1038/ismej.2014.195.
Friendly, M., 2002. Corrgrams: exploratory displays for correlation matrices. Am. Statistician 56, 316–324. https://doi.org/10.1198/000313002533.
G01 Committee, 1999. Practice for Preparing, Cleaning, and Evaluating Corrosion Test Specimens. ASTM International. https://doi.org/10.1520/G0001-90R99E01.
Galushko, A., Kuever, J., 2019. Desulforhopalus. In: Bergey's Manual of Systematics of Archaea and Bacteria. John Wiley & Sons, Ltd, pp. 1–5. https://doi.org/10.1002/9781118960608.gbm01026.pub2.
Ghosh, S., Kain, V., 2010. Microstructural changes in AISI 304L stainless steel due to surface machining: effect on its susceptibility to chloride stress corrosion cracking. J. Nucl. Mater. 403, 62–67. https://doi.org/10.1016/j.jnucmat.2010.05.028.
Gower, J., Young, E., King, S., 2013. Satellite images suggest a new Sargassum source region in 2011. Remote Sensing Letters 4, 764–773. https://doi.org/10.1080/2150704X.2013.796433.
Gray, L.A., Bisonó León, A.G., Rojas, F.E., Veroneau, S.S., Slocum, A.H., 2021. Caribbean-wide, negative emissions solution to sargassum spp. low-cost collection device and sustainable disposal method. Phycology 1, 49–75. https://doi.org/10.3390/phycology1010004.
Gu, T., Wang, D., Lekbach, Y., Xu, D., 2021. Extracellular electron transfer in microbial biocorrosion. Curr. Opin. Electrochem. 29, 100763. https://doi.org/10.1016/j.coelec.2021.100763.
Gudić, S., Vrsalović, L., Matošin, A., Krolo, J., Oguzie, E.E., Nagode, A., 2023. Corrosion behavior of stainless steel in seawater in the presence of sulfide. Appl. Sci. 13, 4366. https://doi.org/10.3390/app13074366.
Guezennec, J., 1990. La biocorrosion. Processus caractéristiques et moyens d'études. Matériaux Techn. 78, 3–8. https://doi.org/10.1051/mattech/199078120003.
Hedrich, S., Schlömann, M., Johnson, D.B., 2011. The iron-oxidizing proteobacteria. Microbiology 157, 1551–1564. https://doi.org/10.1099/mic.0.045344-0.
Herrera, L.K., Videla, H.A., 2009. Role of iron-reducing bacteria in corrosion and protection of carbon steel. Int. Biodeterior. Biodegrad. 63, 891–895. https://doi.org/10.1016/j.ibiod.2009.06.003.
Hervé, V., Lambourdière, J., René-Trouillefou, M., Devault, D.A., Lopez, P.J., 2021. Sargassum differentially shapes the microbiota composition and diversity at coastal tide sites and inland storage sites on caribbean islands. Front. Microbiol. 12, 701155. https://doi.org/10.3389/fmicb.2021.701155.
Heydorn, A., Nielsen, A.T., Hentzer, M., Sternberg, C., Givskov, M., Ersbøll, B.K., Molin, S., 2000. Quantification of biofilm structures by the novel computer program comstat. Microbiology 146, 2395–2407. https://doi.org/10.1099/00221287-146-10-2395.
James, M.N., Hattingh, D.G., 2015. Case studies in marine concentrated corrosion. Eng. Failure Anal. 47, 1–15. https://doi.org/10.1016/j.engfailanal.2014.08.013.
Javaherdashti, R., 2008. Microbiologically Influenced Corrosion, Engineering Materials and Processes. Springer, London, London. https://doi.org/10.1007/978-1-84800-074-2.
Jia, R., Yang, D., Xu, D., Gu, T., 2017. Electron transfer mediators accelerated the microbiologically influence corrosion against carbon steel by nitrate reducing Pseudomonas aeruginosa biofilm. Bioelectrochemistry 118, 38–46. https://doi.org/10.1016/j.bioelechem.2017.06.013.
Jin, Z.H., Ge, H.H., Lin, W.W., Zong, Y.W., Liu, S.J., Shi, J.M., 2014. Corrosion behaviour of 316L stainless steel and anti-corrosion materials in a high acidified chloride solution. Appl. Surf. Sci. 322, 47–56. https://doi.org/10.1016/j.apsusc.2014.09.205.
Kabil, O., Vitvitsky, V., Banerjee, R., 2014. Sulfur as a signaling nutrient through hydrogen sulfide. Annu. Rev. Nutr. 34, 171–205. https://doi.org/10.1146/annurev-nutr-071813-105654.
Keresztes, Z., Felhősi, I., Kálmán, E., 2001. Role of redox properties of biofilms in corrosion processes. Electrochim. Acta 46, 3841–3849. https://doi.org/10.1016/S0013-4686(01)00671-5.
Köchling, T., Sanz, J.L., Gavazza, S., Florencio, L., 2015. Analysis of microbial community structure and composition in leachates from a young landfill by 454 pyrosequencing. Appl. Microbiol. Biotechnol. 99, 5657–5668. https://doi.org/10.1007/s00253-015-6409-4.
Kooli, W.M., Comensoli, L., Maillard, J., Albini, M., Gelb, A., Junier, P., Joseph, E., 2018. Bacterial iron reduction and biogenic mineral formation for the stabilisation of corroded iron objects. Sci. Rep. 8, 764. https://doi.org/10.1038/s41598-017-19020-3.
Koschorreck, M., 2008. Microbial sulphate reduction at a low pH: microbial sulphate reduction at low pH. FEMS (Fed. Eur. Microbiol. Soc.) Microbiol. Ecol. 64, 329–342. https://doi.org/10.1111/j.1574-6941.2008.00482.x.
Kuang, F., Wang, J., Yan, L., Zhang, D., 2007. Effects of sulfate-reducing bacteria on the corrosion behavior of carbon steel. Electrochim. Acta 52, 6084–6088. https://doi.org/10.1016/j.electacta.2007.03.041.
Lanneluc, I., Langumier, M., Sabot, R., Jeannin, M., Refait, P., Sablé, S., 2015. On the bacterial communities associated with the corrosion product layer during the early stages of marine corrosion of carbon steel. Int. Biodeterior. Biodegrad. 99, 55–65. https://doi.org/10.1016/j.ibiod.2015.01.003.
Latosov, E., Loorits, M., Maaten, B., Volkova, A., Soosaar, S., 2017. Corrosive effects of H 2 S and NH 3 on natural gas piping systems manufactured of carbon steel. Energy Proc. 128, 316–323. https://doi.org/10.1016/j.egypro.2017.08.319.
Lee, J.-W., Nam, J.-H., Kim, Y.-H., Lee, K.-H., Lee, D.-H., 2008. Bacterial communities in the initial stage of marine biofilm formation on artificial surfaces. J. Microbiol. 46, 174–182. https://doi.org/10.1007/s12275-008-0032-3.
Li, D.G., Wang, J.D., Chen, D.R., Liang, P., 2014. Influences of pH value, temperature, chloride ions and sulfide ions on the corrosion behaviors of 316L stainless steel in the simulated cathodic environment of proton exchange membrane fuel cell. J. Power Sources 272, 448–456. https://doi.org/10.1016/j.jpowsour.2014.06.121.

Li, X., Duan, J., Xiao, H., Li, Y., Liu, H., Guan, F., Zhai, X., 2017. Analysis of bacterial community composition of corroded steel immersed in sanya and xiamen seawaters in China via method of Illumina MiSeq sequencing. Front. Microbiol. 8, 1737. https://doi.org/10.3389/fmicb.2017.01737.

Li, Y., Feng, S., Liu, H., Tian, X., Xia, Y., Li, M., Xu, K., Yu, H., Liu, Q., Chen, C., 2020. Bacterial distribution in SRB biofilm affects MIC pitting of carbon steel studied using FIB-SEM. Corrosion Sci. 167, 108512. https://doi.org/10.1016/j.corsci.2020.108512.

Li, Z., Yang, J., Lu, S., Dou, W., Gu, T., 2024. Stress corrosion cracking failure of X80 carbon steel U-bend caused by *Desulfovibrio vulgaris* biocorrosion. J. Mater. Sci. Technol. 174, 95–105. https://doi.org/10.1016/j.jmst.2023.07.032.

Lien, T., Madsen, M., Steen, I.H., Gjerdevik, K., 1998. Desulfobulbus rhabdoformis sp. nov., a sulfate reducer from a water-oil separation system. Int. J. Syst. Evol. Microbiol. 48, 469–474. https://doi.org/10.1099/00207713-48-2-469.

Little, B.J., Hinks, J., Blackwood, D.J., 2020. Microbially influenced corrosion: towards an interdisciplinary perspective on mechanisms. Int. Biodeterior. Biodegrad. 154, 105062. https://doi.org/10.1016/j.ibiod.2020.105062.

Little, B.J., Lee, J.S., 2007. Microbiologically Influenced Corrosion, Wiley Series in Corrosion. Wiley-Interscience, Hoboken, N.J.

Liu, Hongwei, Fu, C., Gu, T., Zhang, G., Lv, Y., Wang, H., Liu, Hongfang, 2015. Corrosion behavior of carbon steel in the presence of sulfate reducing bacteria and iron oxidizing bacteria cultured in oilfield produced water. Corrosion Sci. 100, 484–495. https://doi.org/10.1016/j.corsci.2015.08.023.

López-Contreras, A.M., Núñez Valenzuela, P., Celis García, B., Driegen, J., Huerta Lwanga, E., Domin, P., Polett Gurrola, M., Rosas-Luis, R., Verde Gómez, Y., de Vrije, T., 2022. Sargassum in Mexico: from environmental problem to valuable resource. Wageningen Food Biobased Res. Wageningen. https://doi.org/10.18174/574423.

Lu, S., Liu, S., Xue, N., Li, K., Chen, S., Zhu, H., Liu, G., Dou, W., 2024a. Fe0-to-microbe electron transfer corrosion of EH36 steel by planktonic cells of *Desulfovibrio vulgaris* mediated by riboflavin. Corrosion Sci. 236, 112251. https://doi.org/10.1016/j.corsci.2024.112251.

Lu, S., Zhu, H., Xue, N., Chen, S., Liu, G., Dou, W., 2024b. Acceleration mechanism of riboflavin on Fe0-to-microbe electron transfer in corrosion of EH36 steel by *Pseudomonas aeruginosa*. Sci. Total Environ. 939, 173613. https://doi.org/10.1016/j.scitotenv.2024.173613.

Ma, Y., Zhang, Y., Zhang, R., Guan, F., Hou, B., Duan, J., 2020. Microbiologically influenced corrosion of marine steels within the interaction between steel and biofilms: a brief view. Appl. Microbiol. Biotechnol. 104, 515–525. https://doi.org/10.1007/s00253-019-10184-8.

Magoč, T., Salzberg, S.L., 2011. FLASH: fast length adjustment of short reads to improve genome assemblies. Bioinformatics 27, 2957–2963. https://doi.org/10.1093/bioinformatics/btr507.

Marchal, R., 1999. Rôle des bactéries sulfurogènes dans la corrosion du fer. Oil Gas Sci. Technol. -revue De L Institut Francais Du Petrole 54, 649–659. https://doi.org/10.2516/ogst:1999054.

Martin, L.M., Taylor, M., Huston, G., Goodwin, D.S., Schell, J.M., Siuda, A.N.S., 2021. Pelagic Sargassum morphotypes support different rafting motile epifauna communities. Mar. Biol. 168, 115. https://doi.org/10.1007/s00227-021-03910-2.

Melchers, R.E., 2004. Effect of small compositional changes on marine immersion corrosion of low alloy steels. Corrosion Sci. 46, 1669–1691. https://doi.org/10.1016/j.corsci.2003.10.004.

Mendez-Tejeda, R., Rosado, J., Gladys, A., 2019. Influence of climatic factors on Sargassum arrivals to the coasts of the Dominican Republic. J. Oceanogr. Mar. Sci. 10, 22–32. https://doi.org/10.5897/JOMS2019.0156.

Mercier-Bion, F., Yoanna, Leon, Delphine, Neff, Laurent, Urios, Charles, Wittebroodt, Margot, Flachet, Philippe, Dillmann, 2016. Effet des bactéries sur la corrosion d'un acier en contexte nucléaire : caractérisation par une approche multi-techniques (microscopie optique, μ Raman et MEB-EDS). Matériaux Tech. 104, 511. https://doi.org/10.1051/mattech/2017019.

Mukherjee, J., Wong, K.K.W., Chandramouli, K.H., Qian, P.-Y., Leung, P.T.Y., Wu, R.S.S., Thiyagarajan, V., 2013. Proteomic response of marine invertebrate larvae to ocean acidification and hypoxia during metamorphosis and calcification. J. Exp. Biol. 216, 4580–4589. https://doi.org/10.1242/jeb.094516.

Murugan, V.K., Mohanram, H., Budanovic, M., Latchou, A., Webster, R.D., Miserez, A., Seita, M., 2020. Accelerated corrosion of marine-grade steel by a redox-active, cysteine-rich barnacle cement protein. npj Mater. Degrad. 4, 1–8. https://doi.org/10.1038/s41529-020-0124-z.

NACE, 2005. Preparation, Installation, Analysis, and Interpretation of Corrosion Coupons in Oilfield Operations.

Olguin-Maciel, E., Leal-Bautista, R.M., Alzate-Gaviria, L., Domínguez-Maldonado, J., Tapia-Tussell, R., 2022. Environmental impact of Sargassum spp. landings: an evaluation of leachate released from natural decomposition at Mexican Caribbean coast. Environ. Sci. Pollut. Res. https://doi.org/10.1007/s11356-022-22123-8.

Oviatt, C.A., Huizenga, K., Rogers, C.S., Miller, W.J., 2019. What nutrient sources support anomalous growth and the recent sargassum mass stranding on Caribbean beaches? A review. Mar. Pollut. Bull. 145, 517–525. https://doi.org/10.1016/j.marpolbul.2019.06.049.

Palanichamy, S., Subramanian, G., Eashwar, M., 2012. Corrosion behaviour and biofouling characteristics of structural steel in the coastal waters of the Gulf of Mannar (Bay of Bengal), India. Biofouling 28, 441–451. https://doi.org/10.1080/08927014.2012.684947.

Phull, B., 2010. Marine corrosion. In: Shreir's Corrosion. Elsevier, pp. 1107–1148. https://doi.org/10.1016/B978-044452787-5.00046-9.

Pineau, S., Sabot, R., Quillet, L., Jeannin, M., Caplat, Ch, Dupont-Morral, I., Refait, Ph, 2008. Formation of the Fe(II–III) hydroxysulphate green rust during marine corrosion of steel associated to molecular detection of dissimilatory sulphite-reductase. Corrosion Sci. 50, 1099–1111. https://doi.org/10.1016/j.corsci.2007.11.029.

Pusparizkita, Y.M., Fardilah, V.A., Aslan, C., Jamari, J., Bayuseno, A.P., 2023. Understanding of low-carbon steel marine corrosion through simulation in artificial seawater. Aimsmates 10, 499–516. https://doi.org/10.3934/matersci.2023028.

Qu, T., Zhao, X., Hao, Y., Zhong, Y., Guan, C., Hou, C., Tang, X., Wang, Y., 2020. Ecological effects of *Ulva prolifera* green tide on bacterial community structure in Qingdao offshore environment. Chemosphere 244, 125477. https://doi.org/10.1016/j.chemosphere.2019.125477.

Refait, P., Pineau, S., Sabot, R., Antony, H., Jeannin, M., 2013. Mécanismes de la corrosion des aciers au carbone en zone de marnage. Matériaux Tech. 101, 501. https://doi.org/10.1051/mattech/2013084.

Resiere, D., Mehdaoui, H., Florentin, J., Gueye, P., Lebrun, T., Blateau, A., Viguier, J., Valentino, R., Brouste, Y., Kallel, H., Megarbane, B., Cabie, A., Banydeen, R., Neviere, R., 2021. Sargassum seaweed health menace in the Caribbean: clinical characteristics of a population exposed to hydrogen sulfide during the 2018 massive stranding. Clin. Toxicol. 59, 215–223. https://doi.org/10.1080/15563650.2020.1789162.

Rodríguez-Martínez, R.E., Medina-Valmaseda, A.E., Blanchon, P., Monroy-Velázquez, L. V., Almazán-Becerril, A., Delgado-Pech, B., Vásquez-Yeomans, L., Francisco, V., García-Rivas, M.C., 2019. Faunal mortality associated with massive beaching and decomposition of pelagic Sargassum. Mar. Pollut. Bull. 146, 201–205. https://doi.org/10.1016/j.marpolbul.2019.06.015.

Ruiz-Luna, H., Porcayo-Calderón, J., Mora-García, A.G., López-Báez, I., Martinez-Gomez, L., Muñoz-Saldaña, J., 2019. Corrosion performance of AISI 304 stainless steel in CO2-saturated brine solution. Prot Met Phys Chem Surf 55, 1226–1235. https://doi.org/10.1134/S2070205119060261.

Said Ahmed, M., Lescop, B., Pellé, J., Rioual, S., Roos, C., Lebrini, M., 2024. Corrosion of carbon steel in a tropical marine environment enhanced by H2S from sargassum seaweed decomposition. Metals 14, 676. https://doi.org/10.3390/met14060676.

Siuda, A.N.S., Blanfuné, A., Dibner, S., Verlaque, M., Boudouresque, C.-F., Connan, S., Goodwin, D.S., Stiger-Pouvreau, V., Viard, F., Rousseau, F., Michotey, V., Schell, J. M., Changeaux, T., Aurelle, D., Thibaut, T., 2024. Morphological and molecular characters differentiate common morphotypes of atlantic holopelagic sargassum. Phycology 4, 256–275. https://doi.org/10.3390/phycology4020014.

Smetacek, V., Zingone, A., 2013. Green and golden seaweed tides on the rise. Nature 504, 84–88. https://doi.org/10.1038/nature12860.

Smith, M., Bardiau, M., Brennan, R., Burgess, H., Caplin, J., Ray, S., Urios, T., 2019. Accelerated low water corrosion: the microbial sulfur cycle in microcosm. npj Mater. Degrad. 3. https://doi.org/10.1038/s41529-019-0099-9.

Starosvetsky, J., Starosvetsky, D., Pokroy, B., Hilel, T., Armon, R., 2008. Electrochemical behaviour of stainless steels in media containing iron-oxidizing bacteria (IOB) by corrosion process modeling. Corrosion Sci. 50, 540–547. https://doi.org/10.1016/j.corsci.2007.07.008.

Sun, L., Xiong, Z., Qiu, J., Zhu, Y., Macdonald, D.D., 2020. Corrosion behavior of carbon steel in dilute ammonia solution. Electrochim. Acta 364, 137295. https://doi.org/10.1016/j.electacta.2020.137295.

Theirlynck, T., Mendonça, I., Engelen, A., Bolhuis, H., Collado-Vides, L., Tussenbroek, B., García-Sánchez, M., Zettler, E., Muyzer, G., Amaral-Zettler, L., 2023. Diversity of the holopelagic sargassum microbiome from the great atlantic sargassum belt to coastal stranding locations. Harmful Algae 122, 102369. https://doi.org/10.1016/j.hal.2022.102369.

Trigodet, F., Larché, N., Morrison, H.G., Jebbar, M., Maignien, L., 2019a. Electroactive bacteria associated with stainless steel ennoblement in seawater. Front. Microbiol. 10. https://doi.org/10.3389/fmicb.2019.00170.

Trigodet, F., Larché, N., Morrison, H.G., Maignien, L., Thierry, D., 2019b. Influence of dissolved oxygen content on the bacteria-induced ennoblement of stainless steels in seawater and its consequence on the localized corrosion risk. Mater. Corros. 70, 2238–2246. https://doi.org/10.1002/maco.201911225.

Usher, K.M., Kaksonen, A.H., Cole, I., Marney, D., 2014. Critical review: microbially influenced corrosion of buried carbon steel pipes. Int. Biodeterior. Biodegrad. 93, 84–106. https://doi.org/10.1016/j.ibiod.2014.05.007.

Valdez, B., Ramirez, J., Eliezer, A., Schorr, M., Ramos, R., Salinas, R., 2016. Corrosion assessment of infrastructure assets in coastal seas. J. Marine Eng. Technol. 15, 124–134. https://doi.org/10.1080/20464177.2016.1247635.

van Tussenbroek, B.I., Hernández Arana, H.A., Rodríguez-Martínez, R.E., Espinoza-Avalos, J., Canizales-Flores, H.M., González-Godoy, C.E., Barba-Santos, M.G., Vega-Zepeda, A., Collado-Vides, L., 2017. Severe impacts of brown tides caused by Sargassum spp. on near-shore Caribbean seagrass communities. Mar. Pollut. Bull. 122, 272–281. https://doi.org/10.1016/j.marpolbul.2017.06.057.

Vaquer-Sunyer, R., Duarte, C.M., 2008. Thresholds of hypoxia for marine biodiversity. Proc. Natl. Acad. Sci. U.S.A. 105, 15452–15457. https://doi.org/10.1073/pnas.0803833105.

Vastra, M., Salvin, P., Roos, C., 2016. MIC of carbon steel in Amazonian environment: electrochemical, biological and surface analyses. Int. Biodeterior. Biodegrad. 112, 98–107. https://doi.org/10.1016/j.ibiod.2016.05.004.

Vigneron, A., Alsop, E.B., Chambers, B., Lomans, B.P., Head, I.M., Tsesmetzis, N., 2016. Complementary microorganisms in highly corrosive biofilms from an offshore oil production facility. Appl. Environ. Microbiol. 82, 2545–2554. https://doi.org/10.1128/AEM.03842-15.

Wakai, S., Eno, N., Mizukami, H., Sunaba, T., Miyanaga, K., Miyano, Y., 2022. Microbiologically influenced corrosion of stainless steel independent of sulfate-reducing bacteria. Front. Microbiol. 13, 982047. https://doi.org/10.3389/fmicb.2022.982047.

Wan, A.H.L., Wilkes, R.J., Heesch, S., Bermejo, R., Johnson, M.P., Morrison, L., 2017. Assessment and characterisation of Ireland's green tides (ulva species). PLoS One 12, e0169049. https://doi.org/10.1371/journal.pone.0169049.

Wang, H., Ju, L.-K., Castaneda, H., Cheng, G., Zhang Newby, B., 2014. Corrosion of carbon steel C1010 in the presence of iron oxidizing bacteria *Acidithiobacillus ferrooxidans*. Corrosion Sci. 89, 250–257. https://doi.org/10.1016/j.corsci.2014.09.005.

Wang, Z., Wang, X., Huang, Y., Hou, B., 2023. Metagenomic insights into nutrient and hypoxic microbial communities at the macrofouling/steel interface leading to severe MIC. npj Mater. Degrad. 7, 1–15. https://doi.org/10.1038/s41529-023-00365-2.

Wei, T., Simko, V., 2010. Corrplot: visualization of a correlation matrix. https://doi.org/10.32614/CRAN.package.corrplot.

Wiener, M.S., Salas, B.V., Quintero-Núñez, M., Zlatev, R., 2006. Effect of H2S on corrosion in polluted waters: a review. Corrosion Engineering. Sci. Technol. 41, 221–227. https://doi.org/10.1179/174327806X132204.

Y, G.A., Mulky, L., 2023. Biofilms and beyond: a comprehensive review of the impact of Sulphate Reducing Bacteria on steel corrosion. Biofouling 39, 897–915. https://doi.org/10.1080/08927014.2023.2284316.

Yin, H., Wu, Y., 2016. Factors affecting the production of volatile organic sulfur compounds (VOSCs) from algal-induced black water blooms in eutrophic freshwater lakes. Water Air Soil Pollut. 227, 356. https://doi.org/10.1007/s11270-016-3061-2.

Zou, Y., Wang, J., Zheng, Y.Y., 2011. Electrochemical techniques for determining corrosion rate of rusted steel in seawater. Corrosion Sci. 53, 208–216. https://doi.org/10.1016/j.corsci.2010.09.011.